Songklanakarin J. Sci. Technol.
40 (5), 993-1001, Sep. - Oct. 2018

http://www.sjst.psu.ac.th

Original Article

Removal of toxic heavy metal ions from water with $LaAlO_3$ perovskite

Wankassama Haron[1], Anurat Wisitsoraat[2], Uraiwan Sirimahachai[1],
and Sumpun Wongnawa[1*]

[1] *Department of Chemistry, Faculty of Science,*
Prince of Songkla University, Hat Yai, Songkhla, 90112 Thailand

[2] *Nanoelectronics and MEMS Laboratory, National Electronics and Computer Technology Center,*
Khlong Luang, Pathum Thani, 12120 Thailand

Received: 25 October 2016; Revised: 26 April 2017; Accepted: 2 June 2017

Abstract

$LaAlO_3$ perovskite was synthesized by the co-precipitation method using metal nitrate and carbonate salts as starting materials. The product was characterized with X-ray diffractometer (XRD), energy dispersive X-ray spectrometer (EDX), scanning electron microscope (SEM), and transmission electron microscope (TEM). The XRD pattern confirmed the formation of perovskite phase. The SEM micrographs showed that perovskite sample consisted of nanosized particles. The application of synthesized perovskite was investigated as an adsorbent for removal of toxic heavy metal ions in water (Cd^{2+} and Pb^{2+}). The adsorption behavior was studied and found to fit with the Langmuir isotherm. The results showed that $LaAlO_3$ perovskite exhibited high efficiency as heavy metal ions remover from contaminated waters. The used adsorbent could be regenerated with EDTA solution and reused with only slightly less efficiency than the fresh sample.

Keywords: $LaAlO_3$ perovskite, cadmium remover, lead remover, heavy metal ions adsorption, water treatment

1. Introduction

Clean water, air, and foods are important to all forms of life to survive on this planet. Sources of clean water come from surface and ground waters which support all of human activities such as drinking, irrigation of crops, industrial utilization, etc. (World Health Organization [WHO], 1997). With the population growth, water pollution becomes a common environmental problem in many places worldwide. Industrial wastewaters contain many heavy metal ions such as $Cu^{2+,}$ Ni^{2+}, Zn^{2+}, Cd^{2+}, and Pb^{2+} (Biswas *et al.*, 2011; Mohapatra *et al.*, 2007). Besides heavy metal ions, dyes are another pollutant discharged from several industrial plants such as textiles, papers, and plastics which use dyes for coloring their products and also produce substantial volumes of wastewater. Many of these dyes and heavy metal ions tend to accumulate in the living organisms causing diseases and disorders (Banat *et al.*, 1996; Rauf *et al.*, 2009; Robinson *et al.*, 2004). Several methods for treatment of heavy metal ions from wastewaters have been known, however, most of them still have some drawbacks (Sharma *et al.*,1994). Metal oxide possesses some properties such as favorably surface area, microporous structure, and having charge-carrier functional group (OH^-), all of which combined making it a good candidate for being used as an adsorbent for removal of heavy metal ions in aqueous solution (Huelin *et al.*,2006; Lee *et al.*,2004). However, solid separation and sludge management after the metal adsorption on oxides is difficult, because the oxides are usually in colloidal form (Eren *et al.*,2011). There have been reports showing that nano-$BaSrO_3$ and nano-$CaTiO_3$ powders had higher adsorption capacity for heavy metal ions than many nanoparticulate metal oxides but drawbacks still were observed. Due to their small size, the particles tended to coacervate and lost activity after adsorption process as well as difficult to be recovered (Zhang *et al.*,

---

*Corresponding author
Email address: sumpun.w@psu.ac.th

2007; 2008). Hence, the search for other materials of higher qualifications for wastewater treatment is still wide open.

Our research group attempted to find a simple route to prepare $LaMO_3$perovskites (M = Al, Fe, Co, Gd) through low calcination temperature that yield high purity perovskite phase and study for their possible applications in various aspects; among them, as heavy metal ions adsorption material. In the first stage, the precursors for $LaMO_3$ were synthesized by coprecipitation from metal nitrate and carbonate salts. The precursors then were calcined at high temperature (conventional method) and at varied lower temperatures to obtain the desired $LaMO_3$perovskites. These perovskites were used in many studies including as an adsorbents for wastewater treatment. With respect to Cd(II) and Pb(II) ions adsorption, we found that $LaAlO_3$ showed the best performance among all four perovskites prepared. Hence, the details of $LaAlO_3$ as an adsorbent for these two heavy metal ions will be given in this report. The adsorption parameters of contact time, initial concentration of metal ions, and pH of solution were investigated. The adsorption behaviors of $LaAlO_3$ for the two heavy metals were studied based on the Langmuir and the Freundlich isotherms. The use of this adsorbent for environmental remediation has several advantages such as simplicity, low cost, no waste, and no environmental pollution compared with other methods. To the best of our knowledge, $LaAlO_3$ perovskite has never been used as an adsorbent for heavy metal ions in water. The closest study was the work by Zhang *et al.*, 2011 in using calcium titanateperovskite for Pb^{2+}, Cd^{2+}, and Zn^{2+}adsorption from water.

2. Materials and Methods

2.1 Synthesis of $LaAlO_3$ perovskite

$LaAlO_3$ perovskite was prepared based on the co-precipitation method reported previously (Villoria *et al.*, 2011) with some modifications. Starting materials for this perovskite were $La(NO_3)_3{\cdot}6H_2O$ and $Al(NO_3)_3{\cdot}6H_2O$. A specific amount of each was dissolved in distilled water to make 1 M solutions. Both solutions (equal volume) were mixed together with vigorous stirring. Then 2 M $K_2CO_3{\cdot}1.5H_2O$ solution, same volume as one of the nitrate solutions, was rapidly added. Small amount of NaOH solution (1M) was added to initiate precipitation. After the precipitation was complete, the precipitate was filtered and washed with distilled water several times until the washed water became neutral (pH =7). The product was then dried at 100 °C for 6 hrs to yield the "precursor" after which it was calcined at 900 °C for 2 hrs to obtain the $LaAlO_3$ perovskite. Lower calcination temperatures were also employed but failed to yield the perovskite phase.

2.2 Characterization techniques

The crystalline phase of $LaAlO_3$ sample was investigated using the X-ray powder diffractometer, Philips PW 3710 (PHILIPS X' Pert MPD) employing Cu Kα (λ = 0.154 nm) radiation and a Ni filter, over the range 2θ=20-80°. The average crystallite size (D) was calculated with the Debye-Scherrer Equation, Equation 1, as follows

$$D = \frac{K.\lambda}{B.\cos\theta} \quad (1)$$

where D is the average crystallite size, K is a dimensionless shape factor with a typical value of about 0.89 but may vary with the actual shape of the crystallite. The λ is the X-ray wavelength, B is the line width at half the maximum intensity (FWHM) after subtracting the instrumental line broadening in radians, and θ is the Bragg angle. The morphology of the $LaAlO_3$ particles was investigated using JEOL JSM – 5800 LV scanning electron microscope (SEM) using high vacuum mode with secondary electron image conditions and electron micrograph technique. The metal constituents of $LaAlO_3$ perovskite were investigated by using dispersive X-ray spectrometer (EDAX), ISIS 300, Oxford, England. The morphology of the $LaMO_3$ particles was examined using scanning electron microscope (SEM: JEOL, JSM – 5800 LV) operated at 20 kV in secondary electron imaging mode and transmission electron microscope (TEM: JEOL, JSM-2010) operated at 200 kV in bright-field mode.

2.3 Adsorption study

In the studies of contact time, initial concentration, and pH for the adsorption of cadmium and lead on $LaAlO_3$ perovskite nanoparticles, the appropriate amounts of sorbate and sorbent (see below) were mixed, stirred at 300 rpm, and allowed to reach the equilibrium. The resultant solution was centrifuged and the supernatant liquids was analyzed by an inductively couple plasma – optical emission spectrometer (ICP-OES). The amount of adsorbed metal ion at equilibrium condition, q_e (mg/g), was calculated using Equation (2),

$$q_e = \frac{(C_0 - C_e).V}{W} \quad (2)$$

where C_0 and C_e are the concentrations before and after adsorption (mg/L), respectively, V is the volume of solution (L), and W is the weight of adsorbent used (g).

2.3.1 Effect of contact time

A 100 mL of 1 mmol /L for Cd^{2+} and Pb^{2+}solution was pipetted into the beaker containing 0.20 g of $LaAlO_3$ at room temperature and was stirred for 1-40 min. The reaction mixture was then filtered and the supernatant was collected. The metal ion concentration in the supernatant was determined by the ICP to obtain the remained metal ion.

2.3.2 Effect of metal ion concentration

Various concentrations (1, 5, 9, 13, 17, 21, and 25 mmol/L) of each metal ion were used. Adsorbent dose was fixed at 0.20 g per 100 mL of metal ion solution.

2.3.3 Effect of pH

A 100 mL of initial concentration at different pH values (pH 1-6 for cadmium and pH 1-4 for lead) was agitated with 0.20 g of adsorbent. The pH was adjusted with HCl or NaOH solution. Higher pH than that stated was not possible due to metal oxides precipitation. (Native pHs of cadmium and lead solutions are dependent on concentrations and decrease as the concentration increase, for example, at 1 mmol/L the pHs are 5.85 and 4.15 while at 25 mmol/L they are 3 and 2, respectively.)

2.4 Recyclability of $LaAlO_3$ adsorbent

After the first use, the used adsorbent was separated from the mixture and tested in the next round of use by allowing it to adsorb metal ions again from new solution. Alternatively, for comparison, the used adsorbent was regenerated by treating it with 0.1 M EDTA solution for about 1 hr. The regenerated particles were dried in an oven and reused for the next adsorption with a new solution.

3. Results and Discussion

3.1 Product characterization

The identity and purity of the product were studied using XRD and EDX techniques. The XRD pattern of the prepared $LaAlO_3$ perovskite is shown in Figure 1(a). The diffraction peaks matched with the hexagonal structure of $LaAlO_3$ perovskite (JCPDS Card No. 85-0848) and free from other unwanted peaks. The average particle size was calculated using Equation 1 to be 75 nm. The perovskite composition was further investigated with EDX where only three elements of La, Al, and O were detected in the EDX pattern, Figure 1(b). Since the detection capability of EDX is rather high, the product prepared in this way may be considered as of high purity perovskite.

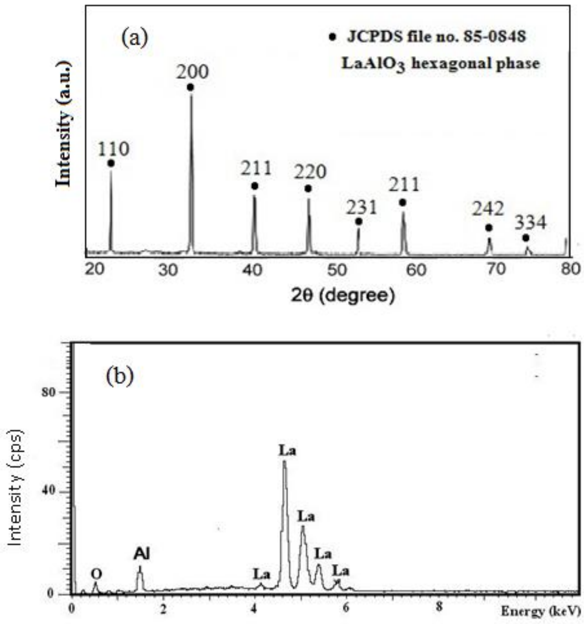

Figure 1. (a) XRD pattern and (b) EDX spectrum of $LaAlO_3$ obtained from 2 hrs of calcination at 900 °C.

3.2 Morphology and surface area

Figure 2(a) shows the scanning electron micrographs of the $LaAlO_3$ samples at 10,000 and 30,000 magnifications. The images show that $LaAlO_3$ powder comprises of mainly rectangular rod-like structures which are several microns long, tens to hundreds of nanometers wide, and tens of nanometer thick. In addition, the nanorod structures display very fine parallel line surface texture. Detailed morphologies of $LaAlO_3$ nanostructures were further investigated using TEM as displayed in Figure 2(b).It is seen that $LaAlO_3$ nanorods with diameters ranging from 30 to 120 nm contains several internal and external bubbles widely distributed throughout the structures. The bubbles are approximately spheroidal and ellipsoidal with varying sizes in the range of 10–80 nm. This unique feature may provide additional surface area beneficial for heavy metal adsorption. The corresponding selected area diffraction (SAED) pattern exhibits broad diffraction rings indicating polycrystalline nature with small grain sizes in nanometer scale. Diffraction rings can be indexed as (101) and (110) planes of $LaAlO_3$ lattice (JCPDS Card No. 85-0848), thus further confirming the hexagonal $LaAlO_3$ structure. The surface area of nano-$LaAlO_3$ based on the N_2 adsorption isotherm was considerably high at 61.7 m^2/g with pore volume of~1.3×10^{-2} cc/g.

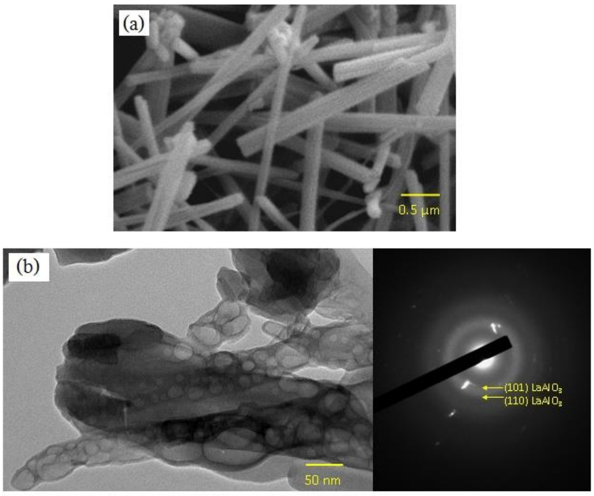

Figure 2. (a) SEM images and (b) Bright-field TEM images and corresponding SAED patterns of $LaAlO_3$ obtained from 2 hrs of calcination at 900 °C.

3.3 Metal ions adsorption

3.3.1 Effect of contact time, metal ion concentration, and pH

The results of contact time and concentrations of both ions to the adsorption on $LaAlO_3$ are shown in Figures 3-4. It can be seen that the amount adsorbed increased with stirring time and reached equilibrium at ~ 1 min. After adsorption experiments, the used adsorbent was recovered and checked with the EDX spectrometer. The resulting EDX spectra showed the presence of both Cd^{2+} and Pb^{2+}indicating

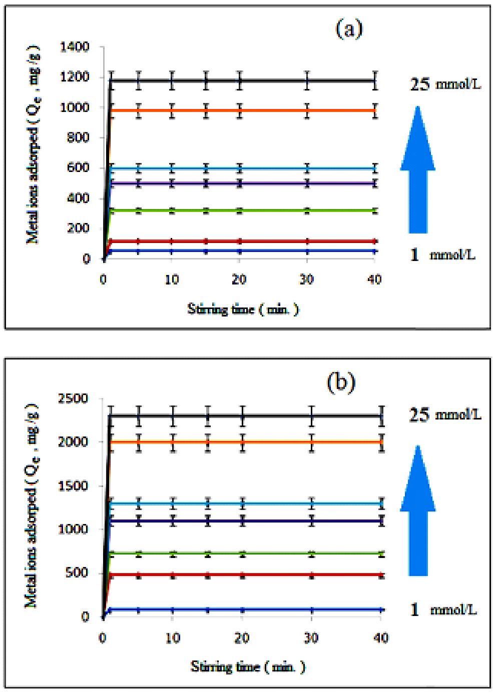

Figure 3. Contact time of Cd^{2+} (a) and Pb^{2+} (b) ions at various concentrations (1, 5, 9, 13, 17, 21, 25 mmol/L) for adsorption on $LaAlO_3$.

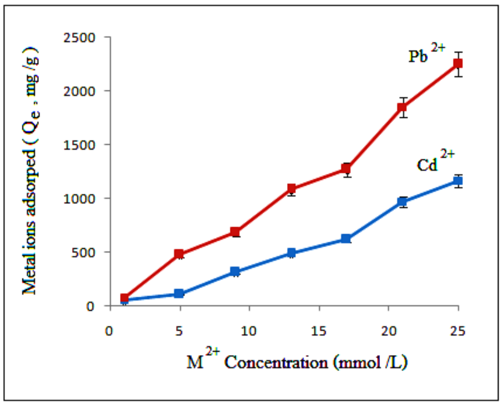

Figure 4. Effect of Cd^{2+} and Pb^{2+} ion concentrations to the adsorption on $LaAlO_3$ (stirring time = 1 min).

the $LaAlO_3$ perovskite adsorbent could really "catch" these two heavy metal ions by adsorption (Figure 5). The elemental mapping associated with each spectrum revealed that the adsorbed metal ions (Cd^{2+}or Pb^{2+}) were distributed evenly on the adsorbent surface.

Figure 6 shows that adsorption of Cd^{2+} and Pb^{2+}ions on $LaAlO_3$ increased with the solution pH because there were more sites for attraction force between positive charge sorbate and negative charge sorbent at higher pH. Normally, the surface of metal oxides were densely covered by positively charged H^+ ions at lower pH range, hence, inhibiting further adsorption of heavy metal ions over it. At higher pH, the H^+ ions were gradually neutralized, hence, favoring the adsorption of heavy metal ions on the adsorbent surfaces.

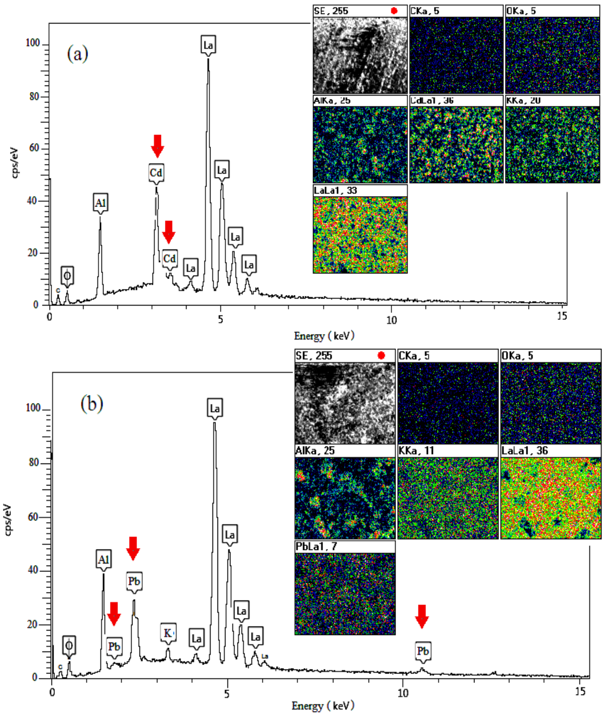

Figure 5. EDX spectra and elemental mapping of $LaAlO_3$ after adsorption of Cd^{2+} (a) and Pb^{2+} (b) ions.

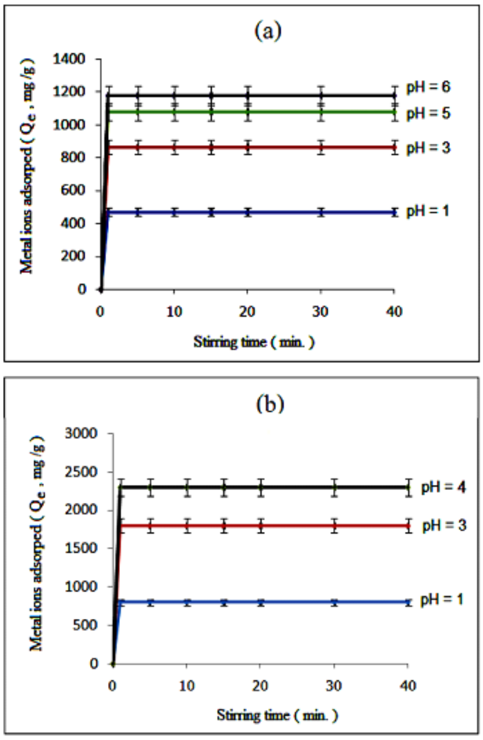

Figure 6. Effect of pH: (a) Cd^{2+} ion and (b) Pb^{2+}ion for adsorption on $LaAlO_3$.

Briefly, we can see that the pH affects the population of active sites on the perovskite surfaces. Note that the ranges of pH under studied were limited to 1-6 for Cd(II) and 1-4 for Pb(II) ions due to precipitation beyond these ranges.

3.3.2 Heavy metal ions adsorption and recyclability

As mentioned in the introduction that $LaAlO_3$ exhibited the highest adsorption for Cd^{2+} and Pb^{2+}ions among the four perovskites prepared in the same series. The q_e of $LaAlO_3$ (at 1 mmol/L) for Cd^{2+} and Pb^{2+}ions were 51.20 and 80.36 mg/g, respectively, which were about double or triple of the rest. The used $LaAlO_3$ adsorbents were investigated for reuses by comparing direct reuse without regeneration and reuse after regeneration (treated with 0.1 M EDTA solution). The results (Figure 7) showed that the regenerated $LaAlO_3$ adsorbent treated with EDTA solution exhibited better performance in reuses than the ones without EDTA treatment. The EDTA treated adsorbent showed only slightly lower efficiency than the freshly prepared powder. EDTA has been known as an excellent chelating ligand for metal ions. When EDTA was used in the regeneration treatment, it effectively formed chelate complexes with Cd^{2+} and Pb^{2+} ions initially adsorbed on the $LaAlO_3$ surface and dissolved into the liquid phase to be drained out later. Note the poor adsorption when the used adsorbents were reused without EDTA regeneration (Figure 7) since the previously adsorbed metal ions still occupied the charged sites on the adsorbent surfaces leaving lower number of charged sites for the next round of reuses. Reuses were conducted in triplicate with very close results and are shown as the bar graphs in Figure 7.

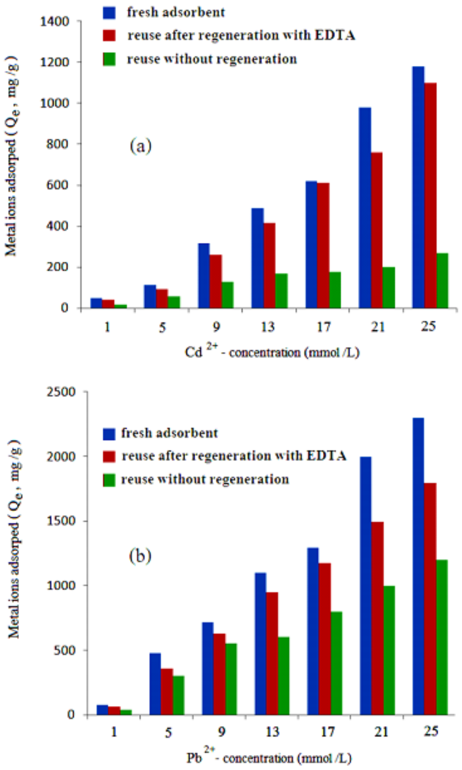

Figure 7. Recyclability of $LaAlO_3$ in concentration range 1-25 mmol /L of metal ions: (a) Cd^{2+} ion and (b) Pb^{2+} ion (eachreuse graph was the average of triplicate runs).

The regeneration with 0.1 M EDTA solution, however, could not completely remove Cd^{2+} and Pb^{2+}ion from the $LaAlO_3$ surface. Trace amount of Cd^{2+} and Pb^{2+} ions were still detected on the adsorbent surface as shown in Figure 8 showing EDX spectra of used adsorbent both before and after regeneration for both metal ions. The remained trace amount on the adsorbent would occupy some active sites; hence, the available active sites would be lower for the next round of reuses. As a result, the efficiency of the reuse of the regenerated adsorbent was slightly lower than the fresh adsorbent as shown in Figure 7.

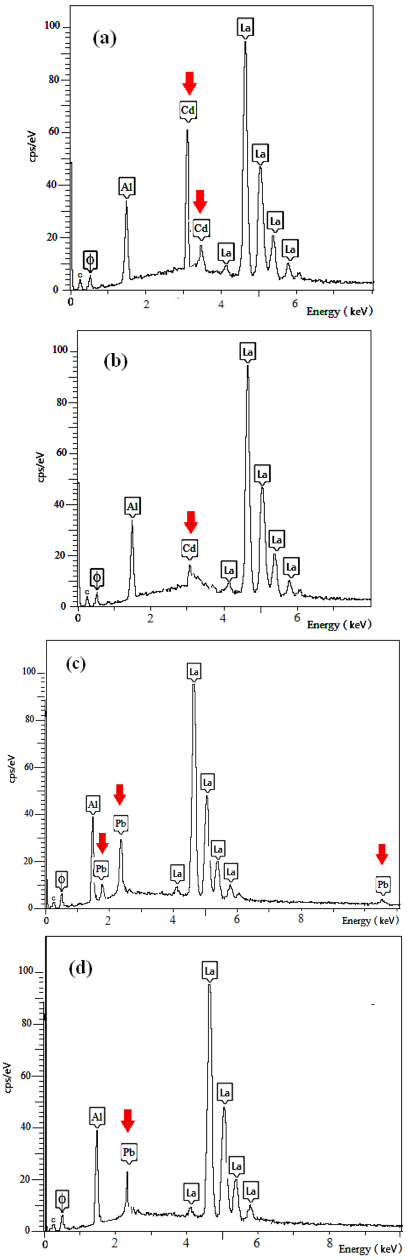

Figure 8. EDX spectra of the reused $LaAlO_3$: (a) after Cd^{2+} ion adsorption, (b) from (a) after being treated with EDTA, (c) after Pb^{2+} ion adsorption, and(d) from (c) after being treated with EDTA.

The reuse efficiencies of $LaAlO_3$ in this work were approximately 80% and 90%for the adsorption of Cd^{2+} and Pb^{2+}, respectively, with the EDTA treatment (0.1M EDTA). Since use of $LaAlO_3$ in this manner has never been reported before, hence, we could only compare this result with other metal oxide adsorbents. Fan *et al*., 2016 have just reported the use of Fe_3O_4 nanoparticle to adsorb Cd^{2+} and Pb^{2+} in water with the efficiency of recyclability ~100% for both the adsorption of Cd^{2+} and Pb^{2+}followed by 0.1M Na_2EDTA treatment. Xie *et al*. (2015) reported the use of CS/ORES-Fe_2O_4 for adsorption of Cd^{2+} in water and reuse with recyclability efficiency of~90 % (also treated with 0.1M Na_2EDTA). Shen *et al*. (2015) reported the synthesis of g-C_3N_4 and used it for Pb^{2+}adsorption and reuses with the recyclability efficiency~90 %.The used g-C_3H_4 was washed with HNO_3 (pH=2) and rinsed with milli-Q water.

3.3.3 Adsorption isotherms

The Langmuir and Freundlich isotherms were used in an attempt to elucidate the adsorption behavior of Cd^{2+} and Pb^{2+} ions on $LaAlO_3$ adsorbent. The Langmuir equation is given as Equation 3:

$$q_e = \frac{q_m.K_L.C_e}{1+K_L.C_e} \quad (3)$$

where K_L is the Langmuir constant (L/mg), q_m is the maximum capacity of adsorbent (mg/g), C_e is the concentrations of metal at equilibrium (mg/L), and q_e is the amount of metals adsorbed at equilibrium (mg/g). The typical of the Langmuir model is monolayer adsorption.

The alternative isotherm is the Freundlich equation which is given as Equation 4:

$$q_e = K_F.C_e^{\frac{1}{n}} \quad (4)$$

where q_e and C_e are defined as above, K_F is indicator of sorption capacity, (1/n) is an empirical parameter relating the adsorption intensity which varies with the heterogeneity of the material. For the value of n, n > 1 indicates that the adsorption process is favorable. The type of adsorption fitting well to the Freundlich equation is multilayer adsorption.

Heavy metal ions (Cd^{2+} and Pb^{2+}) adsorption isotherm data starting at different initial concentrations were investigated and compared to the models of Langmuir and Freundlich. The Langmuir model assumes that adsorption occurs at specific homogeneous sites on the adsorbent and is used successfully in many monolayer adsorption processes.
A linear relationship between the amount of $LaAlO_3$ (g) against the concentration of cadmium (or lead) ions in the remaining solution (mmol/L) was observed (Figure 9). The values of linear correlation coefficients R^2 for the Langmuir model were 0.993 and 0.987 for Cd^{2+} and Pb^{2+}, respectively, while for the Freundlich model, R^2 were 0.987 and 0.892 for Cd^{2+} and Pb^{2+}, respectively, and are summarized in Table 1. From the value of R^2, it can be seen that the Langmuir isotherm is the favored model to explain this adsorption study. The results of R^2 ~1 in the Langmuir model reflects the behavior of the adsorption of Cd^{2+} and Pb^{2+} by $LaAlO_3$as a monolayer adsorption and that no bonding occur between metal ions and surface of adsorbent or metal ions and metal ions.

The results of isotherm study from this work were similar with all of the previous reports by other groups as shown in Table 2 which favored the Langmuir model or only monolayer adsorption for the two metal ions under studied (Cd^{2+} and Pb^{2+}).

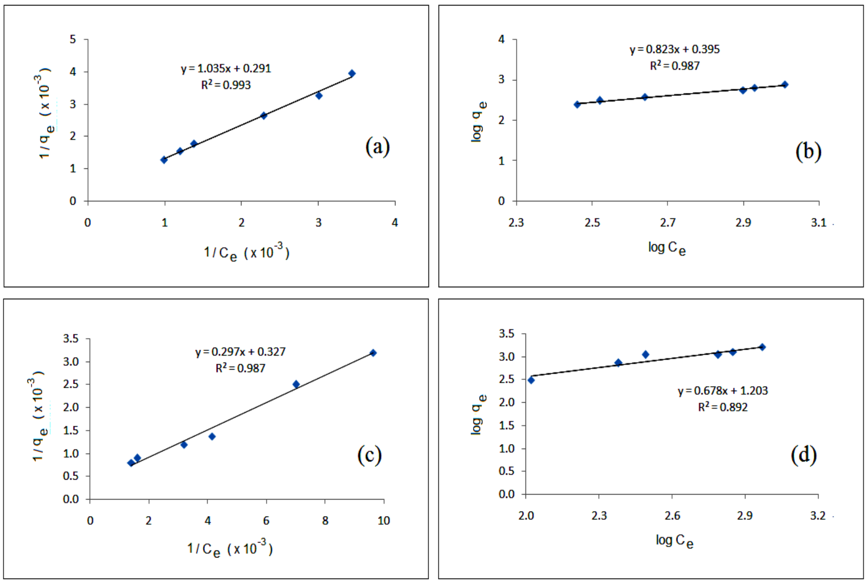

Figure 9. For $LaAlO_3$: (a) and (b) Langmuir isotherm and Freundlich isotherm of Cd^{2+}adsorption, (c) and (d) Langmuir isotherm and Freundlich isotherm of Pb^{2+}adsorption.

Table 1. Langmuir and Freundlich models for Cd^{2+} and Pb^{2+} ions adsorption on $LaAlO_3$.

Metal ions	Langmuir model				Freundlich model			
	Equation	R^2	q_m (mg/g)	K_L	Equation	R^2	n	K_F
Cd^{2+}	y = 1.035x + 0.291	0.993	3.44	0.28	y = 0.823x + 0.395	0.987	1.22	1.48
Pb^{2+}	y = 0.297x + 0.327	0.987	3.06	1.10	y = 0.678x + 1.203	0.892	1.47	3.33

Table 2. Results from adsorption isotherms for Cd^{2+} and Pb^{2+} ions with other adsorbents reported in the literature.

Adsorbents	M^{2+}	Adsorption isotherm				Type of adsorption	Reference
		Langmuir isotherm		Freundlich isotherm			
		R^2	K_L	R^2	K_F		
Nano-Fe_2O_3	Cd^{2+}	0.9976	0.129	0.8342	42.10	Langmuir model	Fan *et al.*, 2016
	Pb^{2+}	0.9932	0.073	0.8462	9.776	Langmuir model	
Gd-doped ZnO	Cd^{2+}	0.9920	0.015	0.9730	2.048	Langmuir model	Ghiloufi *et al.*, 2016
CS/ORES-Fe_2O_4	Cd^{2+}	0.9917	0.070	0.9808	2.950	Langmuir model	Xie *et al.*, 2015
NiO	Pb^{2+}	0.9799	4.210	0.9500	1.540	Langmuir model	Mahmound *et al.*, 2015
g-C_3N_4	Pb^{2+}	0.987	26.68	0.912	3.070	Langmuir model	Ghiloufi *et al.*, 2016

Table 3 is the compilation of q_m values for Cd^{2+} and Pb^{2+} ions with the use of several adsorbents reported in the literatures. These adsorbents can be divided broadly into two types according to their origins: one originated from biological materials; the other from inorganic minerals. The values of q_m in Table 1 for Cd^{2+} and Pb^{2+}ions are higher than many, but not all, adsorbents produced from biological materials. It is worth noting the high value of q_m's exhibited by the adsorbents produced or originated from natural inorganic materials. The high adsorptivity of inorganic adsorbents might be ascribed to the distinct charges on their surfaces. Porosity could be another factor to increase adsorptivity. Unfortunately, $LaAlO_3$ perovskite was found to have very low pore volume (~ 1.3 × 10^{-2} cc/g) so its adsorptivity depends solely on the surface charge without any additional effect to help boost up the adsorption performance.

To the best of our knowledge, the application of $LaAlO_3$ perovskite in the field of adsorption of heavy metal ions has never been reported. $LaAlO_3$, however, has been reported for other uses such as thermo luminescent dosimeter (Hernandez *et al*., 2016) and photoluminescense material (Alves *et al*., 2014; Fu *et al*., 2016).

The information on production cost is scarce; most of the articles just ignore to mention the cost. Take Fe_3O_4 (Fan *et al*., 2016) as an example, using current price list, the cost to synthesize this raw material would be ca. 2,300 Baht/100 g. Surface modification with L-cysteine brought the final product up to ca. 24,000 Baht/100 g due to the high price of L-cysteine. The adsorption capacity of $LaAlO_3$ in this work may not be very high as the best in its class. This problem is limited by the specific surface area of $LaAlO_3$. Further research to increase surface area of $LaAlO_3$ by doping some metal ions may help improve the efficiency of this material for higher metal ions adsorption capacity. From this work, it may be concluded that $LaAlO_3$ is a possible adsorbent for Cd^{2+} and Pb^{2+} removal from wastewater as a result of its environmental and cost benefits.

Table 3. Comparison of q_m values from various adsorbents for Cd^{2+} and Pb^{2+}ions.

M^{2+}	q_m (mg/g)	Adsorbents	References
Biological based adsorbents			
Cd	0.42	Powder of dried carrot residues	(Ata *et al.* 2012)
Pb	0.52		
Cd	0.37	Baker's yeast biomass	(Sulaymon *et al.* 2010)
Pb	0.31		
Cd	36.60	Powder of dried olive tree pruning wastes	(Uzunosmanoglu *et al.* 2011)
Pb	46.20		
Cd	7.19	Almond shells	(Mehrasbi *et al.* 2009)
Pb	8.13		
Cd	7.54	Powder of dried radish peels	(Anwar *et al.* 2009)
Pb	1.23		
Cd	2.88	Activated biocarbon	(Singanan *et al.* 2011)
Pb	2.90		
Inorganic mineral based adsorbents			
Cd	10.37	Polyphosphate-modified kaolinite clay	(Amer *et al.* 2010)
Pb	25.13		
Cd	18.52	Calcite	(Yavuz *et al.* 2007)
Pb	19.92		
Cd	14.61	Chemically treated sodicbentonite clay	(Galindo *et al.* 2013)
Pb	22.79		
Cd	12.05	Modified oil shale ash	(Zhu *et al.* 2012)
Pb	9.41		
Cd	27.44	Calcium alginate beads	(Alfaro *et al.* 2016)
Pb	150.40		
Cd	9.27	RSA clinoptilolite treated with Na^+	(Taenzana, 2011)
Pb	19.84		
Cd	10.82	USA clinoptilolite treated with Na^+	
Pb	4.01		

4. Conclusions

Nanocrystalline of $LaAlO_3$ perovskite was prepared using the co-precipitation method followed by calcination at 900 °C. Lower calcination temperatures were also attempted but could not give the perovskite structure. The product was characterized with XRD, EDX, SEM, TEM, and surface area measurement which revealed significant physical properties of the sample. The sample was studied as an adsorbent for two dreadfully heavy metal ions, i.e., Cd^{2+} and Pb^{2+} ions. Heavy metal ion adsorption isotherm data starting at different initial concentrations were investigated. The adsorption favored the Langmuir isotherm model. The reuse efficiency of $LaAlO_3$ adsorbent was very good as it was only slightly lower than the fresh sample.

Acknowledgements

The authors wish to acknowledge the Office of the Higher Education Commission of Thailand (OHEC) and the Graduate School, Prince of Songkla University, Thailand, for financial support of this work.

References

Alves, N., Ferraz, W. B., & Faria, L. O. (2014). Synthesis and investigation of the luminescent properties of carbon doped lanthanum aluminate ($LaAlO_3$) for application in radiation dosimetry. *Radiation Measurements, 71*, 90-94.

Alfaro-Cuevas-Villanueva, R., Hidalgo-Vazquez, A. R., Pena gos, C. J. C., & Cortes-Martinez, R. (2014). Thermodynamic, kinetic, and equilibrium parameters for the removal of lead and cadmium from aqueous solutions with calcium alginate beads. *The Scientific World Journal, 2014,* Article ID. 647512. doi:10.1155/2014/647512

Ali, R. M., Hamad, H. A., Hussein, M. M., & Malash, G. F. (2016). Potential of using green adsorbent of heavy metal removal from aqueous solutions: Adsorption kinetics, isotherm, thermodynamic, mechanism and economic analysis. *Ecological Engineering, 91*, 317-332.

Amer, M. W., Khalili, F. I., & Awwad, A. M. (2010). Adsorption of lead, zinc and cadmium ions on polyphosphate-modified kaolinite clay. *Journal of Environmental Chemistry and Ecotoxicology, 2*, 1-8.

Anwar, J., Shafique, U., Waheed-uz-Zaman, M. S., & Memoona, M. (2009). Adsorption study of cadmium (II) and lead (II) on radish peels. *Journal of Scientific Research, 39*, 29-34.

Ata, S., Wattoo, F. H., Sidra, L. R., Wattoo, M. H. S., Tirmizi, S. A., & Din, I. (2012). Biosorptive removal of lead and cadmium ions from aqueous solution: The use of carrot residues as low cost no-conventional adsorbent. *Turkish Journal of Biochemistry, 37*, 272-279.

Banat, I. M., Nigam, P., Singh, D., & Marchant, R. (1996). Remediation of dyes in textile effluent: A critical review on current treatment technogies with a propose alternative. *Bioresource Technology, 58*, 217-227.

Biswas, A. K., & Tortajada, C. (2011). Water quality management: An introductory frame work. *Water Resources Management, 27,* 5-11.

Eren, E., & Gumas, H. (2011). Characterization of the structural properties and Pb(II) adsorption behavior of iron oxide coated sepiolite. *Desalination, 273*, 276-284.

Fan, H. L., Li, L., Zhou, S. F., & Liu, Y. Z. (2016). Continuous preparation of Fe_2O_3 nanoparticles combined with surface modification by L-cysteine and their application in heavy metal adsorption. *Ceramics International*, *42*, 4228-4237.

Fu, Z., & Liu, B. (2016). Solution combustion synthesis, photoluminescence and X-ray luminescence of Eu^{3+} -doped $LaAlO_3$ nanophosphors. *Ceramic International, 42*, 2357-2363.

Galindo, L. S. G., Neto, A. F. A., Silva, M. G. C., & Vieira, M. G. A. (2013). Removal of cadmium(II) and lead(II) ions from aqueous phase on sodicbentonite. *Materials Research, 16*, 515-527.

Ghiloufi, I., El Ghoul, J., Modwi, A., & El Mir, L. (2016). Ga-doped ZnO for adsorption of heavy metals from aqueous solution. *Materials Science in Semiconductor Processing, 42,* 102-106.

Hernandez, A. M., Medina, J. Z., Garcia, M. E. C., Nieto, J. A., & Montalvo, T. R. (2016). Synthesis and thermoluminescence of $LaAlO_3{:}Pr^{3+}$ to UVC radiation dosimetry. *Applied Radiation and Isotopes, 118*, 12-17.

Huelin, S. R., Longerich, H. P., Wilton, D. H. C., Fryer, B. J., Li, Y., & Wang, X. 2006. The determination of trace elements in Fe-Mn oxide coatings on pebbles using I.A.- ICP- MS. *Journal of Geochemical Exploration, 91*, 110-124.

Lee, C. I., Yang, W. F., & Hsieh, C. I. (2004). Removal of copper (II) by manganese-coated sand in a liquid fluidized-bed reactor. *Journal of Hazardous Materials, 114*, 45-51.

Mahmoud, A. M., Ibrahim, F. A., Shaban, S. A., & Youssef, N. A. (2015). Adsorption of heavy metal ion from aqueous solution by nickel oxide nano catalyst prepared by different methods. *Egyptian Journal of Petroleum, 24*, 27-35.

Mehrasbi, M. R., Farahmandkia, Z., Taghibeibloo, B., & Taromi, A. (2009). Adsorption of lead and cadmium from aqueous solution by using almond shells. *Water Air and Soil Pollution, 199*, 343-351.

Mohapatra, M., & Anand, S. (2007). Study on sorption of Cd(II) on Tata chromite mine overburden. *Journal of Hazardous Materials, 148*, 553-559.

Rauf, M. A., Qadri, S. M., Ashraf, S., & Al-Mansoori, K. M. (2009). Sorption and desorption of Pb^{2+} ions by dead Sargassum sp. biomass. *Chemical Engineering Journal, 150*, 90-95.

Robinson, T., McMullan, G., Marchant, R., & Nigam, P. (2004). Adsorption studies of toluidine blue from aqueous solution onto gypsum. *Bioresource Technology, 77*, 247-255.

Sharma, D. C., & Forster, C. F. (1994). A preliminary examination into the adsorption of hexavalent chromium using low cost adsorbents. *Bioresource Technology, 47*, 257-264.

Shen, C., Chen, C., Wen, T., Zhao, Z., Wang, X., & Xu, A. (2015). Superior adsorption capacity of g-C_3N_4 for heavy metal ions from aqueous solutions. *Journal of Colloid and Interface Science, 456*, 7-14.

Singanan, M. (2011). Removal of lead(II) and cadmium(II) ions from wastewater using activatedbiocarbon. *Science Asia, 37*, 115-119.

Sulaymon, A. H., Ebrahim, S. E., Al-Musawi, T. J., & Abdullah, S. M. (2010). Removal of lead, cadmium, and mercury ions using biosorption. *Iraqi Journal of Chemical and Petroleum Engineering, 11*, 1-13.

Taenzana, B. (2011). *Adsorption of cadmium, nickel and lead on modified natural zeolite* (Master's research report, Faculty of Engineering and the Built Environment, University of Witwatersrand, Johannesburg, South Africa).

Uzunosmanoglu, O., Uzanik, A., & Engin, M. S. (2011). The removal of cadmium(II), copper(II) and lead(II) from aqueous solutions by olive tree pruning waste. *Fresenius Environmental Bulletin, 20*, 3135-3140.

Villoria, J. A., Alvarez-Galvana, M. C., Al-Zahranib, S. M., Palmisanoc, P., Specchiac, S., & Specchiac, V, (2011). Oxidative reforming of diesel fuel over. $LaCoO_3$perovskite derived catalysts: Influence of perovskite synthesis method on catalyst properties and performance. *Applied Catalysis B: Environmental. 105*, 276-288.

World Health Organization. (1997). *Guidelines for drinking-water quality* (2nd ed.). Geneva, Switzerland: Author.

Xie, M., Zeng, L., Zhang, Q., Kang, Y., Xiao, H., Peng, Y., . . . Luo, J. (2015). Synthesis and adsorption behavior of magnetic microspheres based on chitosan/organic rectorite for low-concentration heavy metal removal. *Journal of Alloys and Compounds, 647*, 892-905.

Yavuz,O., Guzel, R., Aydin, F., Tegin, I., & Ziyadanogullari, R. (2007). Removal of cadmiumand lead from aqueous solution by calcite. *Polish Journal of Environmental Studies, 16*, 467-471.

Zhang, D., Su, H. D., Gao, H., & Liu, J. C. (2007). Adsorption behavior of barium-strontium titanate powder coated by dithizone for lead ion in water. *Acta Chimica Sinica, 65*, 2549-2554.

Zhang, D., Su, H. D., & Gao, H. (2008). Study on adsorption behavior of nanosized barium- strontium titanate powder for lead ion in water using FAAS. *Spectroscopy and Spectral Analysis, 28*, 218-221.

Zhang, D., Su, H. D., & Gao, H. (2008). Study on the adsorption capability of barium-strontiumtitanate powder coated with dithizone for cadmium ion in water. *Spectroscopy and Spectral Analysis, 28*, 693-696.

Zhang, D., Zhan, C. L., & Zhou, P. (2011). Preparation of porous nano-calcium titanate microspheres and its adsorption behavior for heavy metal ion in water. *Journal of Hazardous Materials, 186*, 971-977.

Zhu, B. L., Xiu, Z. M., Liu, N., Bi, H. T., & Lv, C. X. (2012). Adsorption of lead and cadmium ions from oil shale ash. *Oil Shale, 29*, 268-278.